

Influence of Cubic Boron Nitride on the Physical and Mechanical Properties of NAB Alloy Prepared by Powder Metallurgy

Alaa H. Jaafar and Haydar Al-Ethari
Department of Metallurgical Engineering, Materials Engineering College,
University of Babylon, Hillah, Iraq

Abstract: This study focuses on the influence of Cubic Boron Nitride (CBN) particles as reinforcement additive on the properties of Nickel Aluminum Bronze (NAB) alloy of composition Cu-9Al-5Ni-4Fe prepared by powder metallurgy technique. The compact pressure was determined as 700 MPa and the green samples sintered at 930°C for 90 min in vacuum high temperature tube furnace, then heat treated by quenched from 900°C in cold water and tempered at 500°C for 30 min. Cubic boron nitride particles of 0.5, 1, 1.5 and 2 as weights percentage were added as reinforcement particles to the alloy. The influence of the CBN particles on physical, mechanical and elastic properties of the base alloy had been investigated to achieve that the tests included are: XRF test, particle size test, XRD analysis, optical microscope analysis, hardness test, compression test, porosity test, ultrasonic test, thermal conductivity test and coefficient of thermal expansion test. The study showed that the addition of 1.5 wt.% of boron nitride particles has the preferable effect on the mechanical properties where such addition could increase hardness by 59% and compression strength by 16.03%. Experimental results showed that such addition could also increase the elastic properties and porosity and decreased the density, thermal conductivity and coefficient of thermal expansion.

Key words: CBN, NAB, powder metallurgy, elastic properties, density, porosity, hardness

INTRODUCTION

Nickel-Aluminium Bronze (NAB) is a series of copper-based alloy with additions of aluminium, nickel and iron. This alloy shows a good combination of properties such as high strength, good resistance to corrosion and wear which makes it one of the most versatile engineering materials (Jain and Nigam, 2013). Copper with 8-11% Al consists of α phase and a second phase appears at high temperature known as β phase, β phase becomes unstable during cooling and decomposes to α and γ_2 phase as demonstrated in Fig. 1.

γ_2 can be attacked preferentially in seawater and is not desirable. Mechanical properties of NAB alloy have been enhanced due to the addition of nickel and iron to copper-aluminium alloys. Its mechanical properties are improved through the precipitation of several κ phases among α and β phases. NAB alloys are characterized by their excellent corrosion behaviour, partially because Ni and Fe extend the terminal α phase field and suppress the (γ_2) phase formation that occurs in binary Cu-Al alloys as shown in Fig. 2 (Daroonparvar *et al.*, 2011). In the manufacture process of some important industrial and marine pieces of NAB alloy, most pieces are achieved to

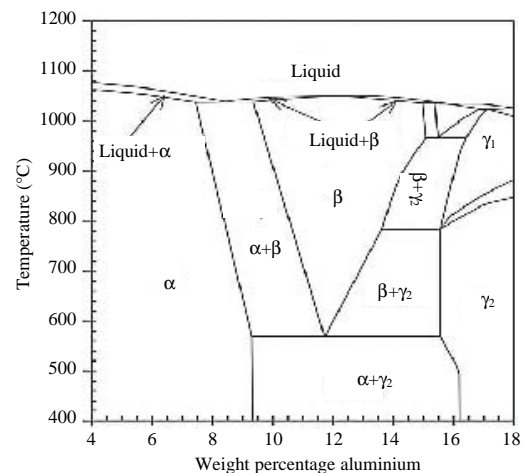


Fig. 1: Phase diagram of copper aluminium alloy

ambient temperature with low cooling rate. Thick parts cool gently to the ambient temperature with little or no mechanical defects. However, thin pieces are cooled by more rate and leads to mechanical damages in the produced parts. The given problems lead to decrease hardness, strength and resistance in alloy. Hardening of

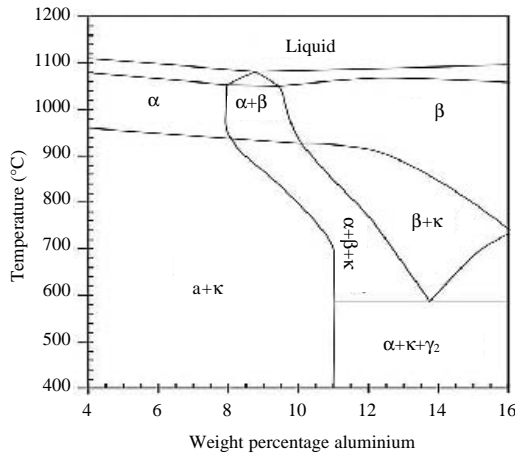


Fig. 2: Phase diagram of NAB alloy

NAB alloy by adding hard ceramic particles is very important issue to improve the mechanical characteristics of the alloy and increase age of NAB pieces (Keshavarz and Abbasi, 2016). Few published attempts studied the hardening of the NAB alloy. Al-Ethari and Hamza (2014) studied the effect of SIC and graphite as reinforcement element on physical, mechanical and machining properties of NAB alloy prepared by powder metallurgy, Keshavarz and Abbasi (2016) studied the improvement of the surface structure of NAB alloy by adding Al₂O₃ nanoparticles using Friction Stir Process (FSP) method, Abbasi-Khazaei and Keshavarz (2017) studied the corrosion properties and microstructure of NAB/Al₂O₃ surface nano composite. In this regard, Cubic Boron Nitride (CBN) is an interesting material owing to its unique combination of properties such as very high hardness, low density, high melting point, high thermal conductivity and high electrical resistivity (Seetharaman *et al.*, 2013).

This research aims to study influence of adding cubic boron nitride particles on some physical and mechanical properties of nickel-aluminium bronze alloy prepared by Powder Metallurgy (P/M). This could be accomplished through studying the effect of a wide percentage range of boron nitride particles as reinforcement to the alloy. Many mechanical and physical tests were carried out to compare between the base alloy and the reinforced composite. These tests include hardness, compression properties, ultrasonic wave, porosity, density, thermal conductivity and coefficient of thermal expansion.

MATERIALS AND METHODS

Tests for basic materials: X-Ray Florescence (XRF) analysis for the used powders was carried out using XRF analyzer type (DS-2000) at General Company for Inspection and Engineering Rehabilitation,

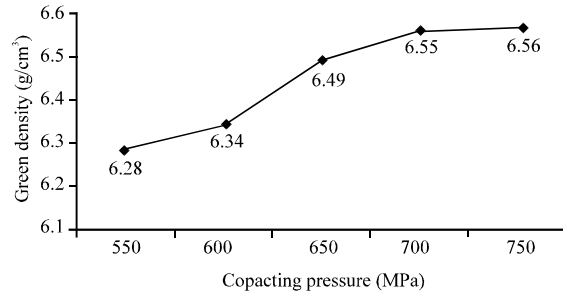


Fig. 3: Effect of compacting pressure on green density of the base alloy samples

Powders	Purity	Average particles size (µm)
Copper	99.10	1.171
Aluminium	99.35	2.341
Nickel	99.27	1.922
Iron	98.70	5.062
Boron nitride	99.50	0.420

Baghdad. Also, particle size analysis was carried out by using laser particle size analyzer type at the University of Babylon/College of Materials Engineering Ceramics and Building Materials Labs (Table 1).

Samples preparation: To study the effect of CBN particles on physical and mechanical properties of NAB alloy with chemical composition of Cu-9%Al-5%Ni-4%Fe according to ASTM B150 (Anonymous, 2003), samples with 0, 0.5, 1, 1.5 and 2 wt.% of CBN particles as a reinforcing element was prepared. A wet mixing was used with 2%wt. of acetone. Mixing process for 6 h was performed by an electrical mixer type STGQM-15-2. Uniaxial compacting via. double action steel die was carried out on electro hydraulic compacting machine type (Channel automatic cube and cylinder compression machines, CT340- CT440, USA), Lubricant was used for the inside walls of the steel die. Three types of samples were prepared. Cylindrical samples with 19 mm in diameter and 12 mm in height are used for testing hardness, microstructure, X-ray and thermal conductivity; samples with a diameter of 9 mm and a height of 13.5 mm are used for compression test according to ASTM B925-08 specifications (Rao *et al.*, 2010) and samples of 10 mm in diameter and 50 mm in height for thermal expansion test and ultrasonic wave tests to measure the elastic properties. The preferred compacting pressure was determined experimentally based on presence of surface cracks of green compact and by determining the pressure that gives the highest green density. Figure 3 demonstrates the increase of the green density with increasing the compacting pressure until it reaches the maximum effect in 700 MPa then slight increase on green density was observed, so, a compacting pressure of 700 MPa was used to prepare all samples.

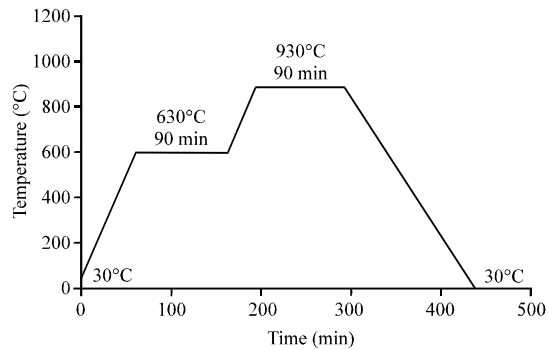


Fig. 4: The sintering program of the green compacts

The sintering process of the green compact samples was achieved via vacuum high temperature tube furnace with a pressure of 10^{-4} torr. The sintering program is shown in Fig. 4. When the sintering program has finished, the samples are left inside the furnace to cool down till the temperature of sintered samples drops to room temperature again. A eat treatment for the sintered samples was carried out by heating to a temperature of 900°C for 50 min with a heating rate of $10^{\circ}\text{C}/\text{min}$, then quenching in cold water and tempered at 500°C for 30 min.

Physical and mechanical tests

Micro-hardness test: Appropriate grinding and polishing were carried out before subjecting the specimens to the test. The test was conducted at micro Vickers hardness device type Digital Micro Vickers Hardness Tester TH 717 using a load of 500 g for 10 sec with a square base diamond pyramid. The hardness was recorded as an average of five readings for each specimen.

Optical microscope test: This test covered sintered and heat treated matrix alloy specimens to investigate the influence of each process on the microstructure of the prepared samples. Appropriate grinding and polishing were carried out for the tested specimens using paper grits as 180, 400, 800, 1000, 1200 and 2000 and polished by using diamond solution with 0.2 mm by using a grinding and polishing machine. Then, they were etched using etching solution consisting of 5 g FeCl_3 , 3 MML of HCl and 92 MML of distilled water at room temperature. Then, all samples were washed by distilled water and dried using electric drier.

X-Ray Diffraction (XRD) analysis: This test covered heat treated matrix and composite specimens by using MiniFlex 2. The analysis had been done at General Company for Inspection and Engineering Rehabilitation, Baghdad. The testing conditions are: target: Cu, wave length of 1.54060 \AA voltage and current are 30 kV and 15 mA, respectively scanning speed 2 deg./min and scanning range of $20\text{-}90^{\circ}$.

Compression test: Specimens with 9 mm in diameter and 13.5 mm in height were prepared for this test. This test was conducted at universal testing machine type (Computer control electronic universal testing machine, model WDW-200 max load capacity 200 kN) with a piston speed of 0.2 mm/min.

Porosity and density test: Based on ASTM B-328 porosity and density of final (quenched and tempered) the samples were determined according to Eq. 1:

$$\text{Final porosity} = \frac{W_w - W_d}{W_{\text{sat}} - W_s} \times 10 \quad (1)$$

$$\text{Final density} (p_a) = \frac{W_d}{W_{\text{sat}} - W_s} \times P_w \quad (2)$$

Where:

W_d = Dry Weight of the specimen (the specimen is dried at 80°C for 4 h under vacuum pressure of 10^{-4} torr then cooled to room temperature inside the furnace, then weighted)

W_w = Wet Weight of the specimen (the specimen was weighted after immersing it for 24 h in distilled water)

W_{sat} = Saturated Weight (the specimen was weighted after immersing it for 5 h in distilled water at 80°C)

W_s = Suspended Weight (weighting the suspended specimen in distilled water)

P_w = Water density determined by knowing its temperature via a mercurial thermometer which is provided by Anonymous (2003)

Thermal conductivity test: Specimen with 19 mm in diameter and 12 mm in height was prepared for matrix and composite samples in order to investigate the thermal conductivity of these samples using thermal coefficient meter type (YBF-3). The sample was placed between the two copper disks, then a required temperature of 100°C was selected to measure the thermal conductivity coefficient based on Fourier 's law:

$$Q = -KA \frac{dt}{dx} \quad (3)$$

Where:

Q = The heat flow (W)

K = The thermal conductivity ($\text{W}/(\text{m}\cdot^{\circ}\text{C})$)

A = The cross sectional area

dt/dx = The temperature gradient in the direction of flow ($^{\circ}\text{C}/\text{m}$)

Thermal expansion test: A quickline-05 thermo-mechanical analysis instrument was used to determine the Thermal Expansion Coefficients (CTE) of the base and composite samples. A heating rate of 15°C/min was maintained. The changes length was recorded every 100 up to 800°C.

Ultrasonic wave test: Samples with 10 mm diameter and 50 mm height were prepared for each matrix and reinforced composite in order to investigate the elastic properties for each samples. Ultrasonic wave device type CCT-4 was used and digital monitor was used to appear the transfer time of ultrasonic wave and can calculate the longitudinal and transverse velocity. Elastic modulus, Poisson's ratio and shear modulus can obtain by applying the longitudinal and transverse velocity values as in Eq. 4-6 (Kumar *et al.*, 2009):

$$v = 1 - 2 \frac{V_T}{V_L} \quad (4)$$

$$E = V_L^2 \rho (1 + \sigma)(1 - 2\sigma) / (1 - \sigma) \quad (5)$$

$$G = V_T^2 \rho \quad (6)$$

Where:

V = Poisson's ratio

V_T = Shear (Transverse) Velocity (m/sec)

V_L = Longitudinal Velocity (m/sec)

E = Elastic modulus (GPa)

G = Shear modulus (GPa)

ρ = Density (kg/m³)

RESULTS AND DISCUSSION

Hardness test: Specimen's code and Vickers hardness of the specimens after sintering and heat treatments processes are shown in Table 2.

The results show a significant increase in hardness due to the heat treatment of the samples, these confirm the formation of martensitic β phase which is very hard. The hardness of the NAB is in agreement with previous research (Keshavarz and Abbasi, 2016; Takaloo *et al.*, 2011). With increasing in percentage of CBN the hardness increases significantly, this increment could be attributed to the very high hardness of CBN particles tend to restrain movement of the matrix and act as barriers to dislocation motion, so, the hardness increases. With a percentage of CBN more than 1.5% the improvement in hardness is unremarkable, so this percentage was relied in this study, i.e., all tests will be based on S3 samples.

Table 2: Vickers micro-hardness of the samples prepared

Specimens code	Cubic boron nitrid (%)	Hardness after sintering (kg/mm ²)	Hardness after heat treatment (kg/mm ²)
S0	0.0	148	187
S1	0.5	174	236
S2	1.0	207	276
S3	1.5	242	297
S4	2.0	256	305

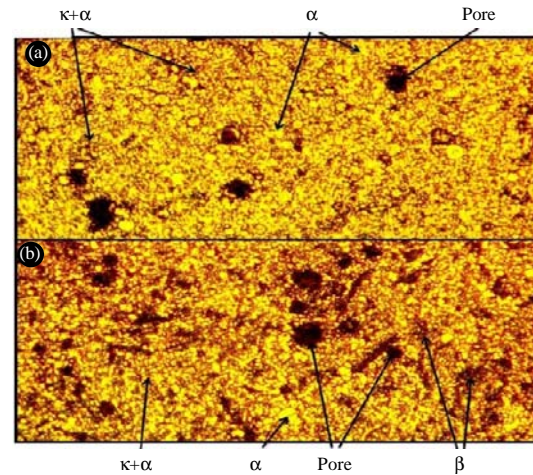


Fig. 5: Microstructure of s0 alloy; a) After sintering and b) After heat treatment

Optical microscope test: Figure 5 illustrates the microstructures of sintered and heat treated matrix alloy where the width of images is 80 μ m.

The microstructure of the sintered alloy insures the formation of the fine κ phases as well as the presence of α phase after the sintering process, the weight percentage of the iron which is <5% explains the absence of the large κ phase. After heat treatments (quenching and tempering) the microstructure introduces retained β which is formed due to the high cooling rate. These results are in agreement with references (Daroonparvar *et al.*, 2011).

X-ray diffraction analysis results: Figure 6 demonstrates the XRD analysis for the heat treated S0 alloy the diffraction patterns prove the formation of κ phases in addition to α phase due to the presence of iron and nickel. The retained β phase could be indicated by the XRD analysis and its presence was insured by the results of the optical microscope examination. The formation of these phases prove the success of the sintering process. The results are in good agreement with the reference (Lv *et al.*, 2015). Figure 7 demonstrates the XRD analysis for the heat treated S3 composite. Figure 7 shows a presence of diffraction pattern belongs to CBN which insures the presence of CBN phase.

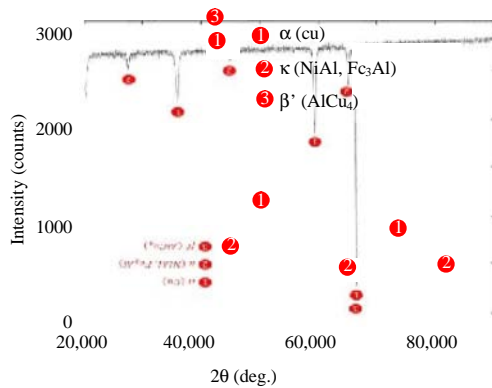


Fig. 6: XRD pattern of heat treated S0 alloy

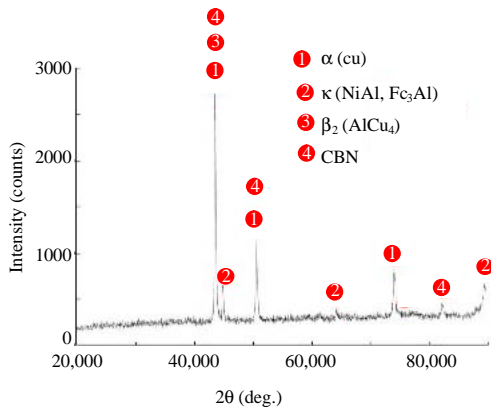


Fig. 7: XRD pattern of heat treated S3 alloy

Compressive test results: The compression strength of S0 and S3 are 481, 558 MPa, respectively which has been improved in composite when compared with the matrix alloy. The strengthening effect of particles in NAB matrix composite is attributed to two factors: the load bearing effect of the reinforcement in which the reinforcement can share the applied stress directly by the stress transfer from the matrix. The dislocation strengthening in the matrix which is related to the nucleation of additional dislocations in the matrix due to the introduction of the reinforcement. The improvement in the compression strength by adding ceramic particles was found in previous research (Scudino *et al.*, 2010).

Porosity and density results: The final density of S0 alloy and S3 composite are 7.38, 7.25 g/cm³, respectively. Generally, CBN has low density in nature, so the density values of the matrix alloy decreased with addition of CBN particles. These decreases in density contributed directly in using of these composites in wide range engineering applications that need lightweight materials.

The density result of the prepared NAB alloy is close to the density of NAB alloy which is 7.59 g/cm³ worked by Daroonparvar *et al.* (2011) with an error of 2.7%. The final porosity of S0 alloy and S3 composite are 9, 10%, respectively. The porosity of the alloy increases with addition of CBN particles, the presence of CBN particles change the normal surface tension, wetting behaviour and deterred the retention of air bubble within the samples.

Thermal conductivity results: The thermal conductivity value of the S0 alloy and S3 composite are equal to 37, 36 W/m.°C, respectively. A decrease by 8% in the thermal conductivity of composite compared with NAB alloy due to the low thermal conductivity of the CBN particles which impede the heat transfers through the material. The porosity generated by the reinforcing particles also can be a factor that reduces the thermal conductivity.

The thermal conductivity of the prepared NAB alloy seems to be lower than the thermal conductivity of cast NAB alloy 42 W/m.°C (Daroonparvar *et al.*, 2011), this is due to the presence of the closed pores which contain low thermal conductivity gas.

Thermal expansion results: The coefficient of thermal expansion for both matrix alloy S0 and composite S3 was obtained to be 15.3, 15.1×10⁻⁶/°C, respectively. The results indicate an improvement in dimensional stability (reduction in the Coefficient of Thermal Expansion (CTE) values) through the addition of CBN particles in very small fraction and this is due to the low thermal expansion of the CBN particles compared with the thermal expansion of the matrix alloy. The thermal expansion of the prepared NAB alloy is close to the thermal expansion of the NAB alloy 17×10⁻⁶/°C according to Daroonparvar *et al.* (2011).

Ultrasonic wave test results: The longitudinal and transverse velocity of ultrasonic wave for matrix alloy are 1540, 800 m/sec, respectively and for S3 the are 1600, 840 m/sec, respectively. Hence, Poisson's ratio, elastic modulus and shear modulus can be determined based on Eq. 4-6, respectively and the results are demonstrated in Table 3.

The results show an improvement in the elastic modulus and shear modulus, these improvements attributed to the role of CBN particles which served as obstacles impeded the dislocation motion thereby strengthened the matrix and increase the modulus. The Poisson's ratio of the composite decreases in compared

Table 3: Elastic properties S0 and S3 materials

Samples code	Elastic modulus (GPa)	Shear modulus (GPa)	Poisson's ratio
S0	122	47	0.3152
S3	131	51	0.3100

Table 4: Physical and mechanical properties of matrix and composite materials with change percentage

Properties	S0	S3	Change (%)
Micro-hardness (kg/mm ²)	1870	297	59
Compression strength (MPa)	4810	558	16
Porosity	9000	11	11
Density (g/cm ³)	7.38	7.25	20
Thermal conductivity (W/m.°C)	3700	36	30
Coefficient of thermal expansion (10 ⁻⁶ /°C)	15.3	15.1	10
Poisson's ratio	0.3152	0.3100	20
Elastic modulus (GPa)	12200	131	70
Shear modulus (GPa)	47.00	51	12

with the matrix alloy because the reinforced particles work to decrease ductility as result, decrease the transverse strain to longitudinal strain ratio. The elastic properties of the prepared NAB alloy are close to the elastic properties of NAB alloy as demonstrated by Daroonparvar *et al.* (2011).

Abbreviation of mechanical and physical

Properties results: The mechanical and physical properties of the matrix and reinforced composite and the percentage change in these properties are shown in Table 4.

CONCLUSION

According to the results of the present research, the following can be concluded: cubic boron nitride is very hard, lightweight and can serve effectively as reinforcement in metal matrix composite.

Most of mechanical properties are significantly enhanced with addition of CBN particles to NAB matrix. Samples of NAB alloy can be prepared by sintering the compacted constituting powders at 930°C for 90 min and quenching in water after heating to 900°C for 50 min and aging at 500°C for a period of 30 min. Powder metallurgy is a successful method in manufacturing of metal matrix composites.

ACKNOWLEDGEMENT

Researchers are thankful to the staff of the Researchshop Materials Lab. in Babylon University.

REFERENCES

Abbasi-Khazaei, B. and S. Keshavarz, 2017. Nickel-aluminum-bronze/Al₂O₃ surface nanocomposite produced by friction-stir processing: Corrosion properties and microstructure. *Mater. Corros.*, 68: 883-891.

Al-Ethari, H.A. and H. Hamza, 2014. Tool life modeling for drilling NAB alloy reinforced by SiC and graphite. *Intl. J. Eng. Innovative Technol.*, 3: 13-17.

Anonymous, 2003. Density, oil content and interconnected porosity of sintered metal structural parts and oil-impregnated bearings. ASTM International designation B 328-96, West Conshohocken, Pennsylvania, USA.

Daroonparvar, M.R., M.M. Atabaki and A. Vakilipour, 2011. Effect of pre-heat treatment on corrosion behavior of nickel-aluminium bronze alloy. *Metalurgija*, 17: 183-198.

Jain, P. and P.K. Nigam, 2013. Influence of heat treatment on microstructure and hardness of nickel aluminium bronze (Cu-10Al-5Ni-5Fe). *J. Mech. Civ. Eng.*, 6: 16-21.

Keshavarz, S. and K. Abbasi, 2016. Improvement the surface structure of Nickel Aluminum Bronze (NAB) alloy using Al₂O₃ nanoparticles and FSP method. *Am. J. Oil Chem. Technol.*, 4: 4-13.

Kumar, S.S., V.S. Bai, K.V. Rajkumar, G.K. Sharma and T. Jayakumar *et al.*, 2009. Elastic modulus of Al-Si/SiC metal matrix composites as a function of volume fraction. *J. Phys. D Appl. Phys.*, 42: 1-10.

Lv, Y., L. Wang, X. Xu and W. Lu, 2015. Effect of post heat treatment on the microstructure and microhardness of friction stir processed NiAl bronze (NAB) alloy. *Met.*, 5: 1695-1703.

Rao, J.B., D.V. Rao and N.R.M.R. Bhargava, 2010. Development of light weight ALFA composites. *Intl. J. Eng. Sci. Technol.*, 2: 50-59.

Scudino, S., F. Ali, K.B. Surreddi, K.G. Prashanth and M. Sakaliyska *et al.*, 2010. Al-based metal matrix composites reinforced with nanocrystalline Al-Ti-Ni particles. *J. Phys. Conf. Ser.*, 240: 1-5.

Seetharaman, S., J. Subramanian, K.S. Tun, A.S. Hamouda and M. Gupta, 2013. Synthesis and characterization of nano boron nitride reinforced magnesium composites produced by the microwave sintering method. *Mater.*, 6: 1940-1955.

Takaloo, A.V., M.R. Daroonparvar, M.M. Atabaki and K. Mokhtar, 2011. Corrosion behavior of heat treated nickel-aluminum bronze alloy in artificial seawater. *Mater. Sci. Appl.*, 2: 1542-1555.